Phase transition of anisotropic frustrated Heisenberg model on the square lattice

Ai-Yuan Hu[1] and Huai-Yu Wang[2,*]

[1]*College of Physics and Electronic Engineering, Chongqing Normal University, Chongqing 401331, China*

[2]*Department of Physics, Tsinghua University, Beijing 100084, China*

(Received 27 September 2015; revised manuscript received 15 December 2015; published 11 January 2016)

We have investigated the J_1-J_2 Heisenberg model with exchange anisotropy on a square lattice and focused on possible AF1-AF2 phase transition below the Néel point and its dependence on the exchange anisotropy, where AF1 and AF2 represent Néel state and collinear state, respectively. We use the double-time Green's-function method and adopt the random-phase approximation. The less the exchange anisotropy, the stronger the quantum fluctuation of the system will be. Both the Néel state and collinear state can exist and have the same Néel temperature for arbitrary anisotropy and spin quantum number S when $J_2/J_1 = 0.5$. Under such parameters, the calculated free energies show that there may occur a first-order phase transition between the Néel state and collinear state for an arbitrary S when anisotropy is not strong.

DOI: 10.1103/PhysRevE.93.012108

I. INTRODUCTION

The antiferromagnetic systems described by the J_1-J_2 Heisenberg exchange Hamiltonian on the square lattice have been investigated by many researchers [1]. The Hamiltonian of the J_1-J_2 model reads

$$H = J_1 \sum_{\langle i,j\rangle} S_i \cdot S_j + J_2 \sum_{[i,j]} S_i \cdot S_j, \tag{1}$$

where S_i is the spin at site i. J_1 and J_2 are the nearest-neighbor (NN) and next-nearest-neighbor (NNN) antiferromagnetic (AF) exchange interactions, respectively. The sums in the first and second terms in Eq. (1) run over the NN and NNN spin pairs, respectively. For $J_2 = \mathbf{0}$, the Hamiltonian is an ordinary NN AF system with Néel order, i.e., all the NN spins are antiparallel to each other. When $J_2 \neq 0$, the Hamiltonian is the so-called J_1-J_2 model, and the magnetic properties of the system depend on J_2. In this model, the strong frustration is induced by the NNN AF exchange, which may break the Néel order. The frustration is caused by the mutual competition between J_1 and J_2, which can trigger a rich phase diagram [1–10].

The investigations indicated that for a two-dimensional square lattice a Néel state (AF1) was envisaged at $J_2/J_1 \leqslant 0.5$, while a collinear state (AF2) should develop for $J_2/J_1 \geqslant 0.5$ [3–12]. The AF1 was characterized by an antiparallel alignment of NN spins with a corresponding magnetic wave vector $Q_{\mathrm{AF1}}(\pi,\pi)$. The AF2 was twofold degenerated and the corresponding magnetic wave vectors are $Q^1_{\mathrm{AF2}}(\pi,0)$ and $Q^2_{\mathrm{AF2}}(0,\pi)$, which are characterized by the fact that the NN spins take a parallel orientation in the vertical (horizontal) direction and an antiparallel orientation in the horizontal (vertical) direction, respectively. The magnetic wave vector Q gives a classical description of the magnetic order. However, in this paper, we study the quantum behavior of the system.

There might occur transition between the AF1 and AF2 states. The phase transition may be sensitive to anisotropy. It is well known that for isotropic two-dimensional magnetic systems there was no long-range order at finite temperature [13], but at zero temperature the ordering can occur and depends on the Hamiltonian. For the two-dimensional J_1-J_2 model, the AF1 and AF2 configurations exist at small and large J_2 value, respectively, separated by an intermediate quantum paramagnetic phase (see, e.g., [7], and references cited therein). Nevertheless, an anisotropy, no matter how faint, would cause a long-range order at finite temperature [4,5].

Numerous efforts have been focused on the transition points in the J_1-J_2 square-lattice antiferromagnet. For instance, for the isotropy case, the key question is to obtain the precise values of the ground-state transition point subject to the competition between J_1 and J_2 [1,14–18]. For the anisotropy case, the investigative emphasis is to discuss the effect of anisotropy on the phase diagram [2–10]. However, compared to the case of zero temperature, the discussion about the case of finite temperature appears to be much less. There may be some interesting features still hidden in the cases of finite temperature.

Motivated by that, we will study the magnetic properties of the two-dimensional J_1-J_2 model with an exchange anisotropy at finite temperatures by means of the many-body Green's-function method under the random-phase approximation (RPA). Our results show that both the AF1 and AF2 states can exist and have the same critical temperature for arbitrary anisotropy and spin quantum number S at finite temperature when $J_2/J_1 = 0.5$. The calculated free energies show that there can occur a phase transition between the two states below the critical point for appropriate anisotropic parameters, and the internal energies indicate that this is a first-order transition.

This paper is organized as follows. In Sec. II, after introducing the Hamiltonian, we present the formulism of the Green's function and establish the self-consistent equation for evaluation of magnetizations. In Sec. III, the numerical results are presented and discussed. Section IV presents our conclusions.

II. HAMILTONIAN AND METHOD

Our two-dimensional anisotropic J_1-J_2 Heisenberg antiferromagnets model is described by the following Hamiltonian:

$$H = J_1 \sum_{\langle i,j\rangle} \left[S_i^z S_j^z + \eta\left(S_i^x S_j^x + S_i^y S_j^y\right)\right] + J_2 \sum_{[i,j]} \left[S_i^z S_j^z + \eta\left(S_i^x S_j^x + S_i^y S_j^y\right)\right], \tag{2}$$

*wanghuaiyu@mail.tsinghua.edu.cn

where S_i^x, S_i^y, and S_i^z represent the three components of the spin-S operator for a spin at site i, and η denotes the anisotropic parameter with $0 \leqslant \eta \leqslant 1$. In this paper, our primary purpose is to study the magnetic properties of the system at finite temperature. When $\eta = 1$, the model is isotropic, and there will be no long-range order at finite temperature [13]. Thus we consider the cases when $\eta < 1$. The exchange anisotropy did appear in real materials [11,19,20]. Therefore, the study of the Hamiltonian Eq. (1) is meaningful. For the sake of convenience, we let Boltzmann constant $k_B = 1$ so that all the quantities—including exchange parameters, temperature T, and sublattice magnetization $m = \langle S^z \rangle$—become dimensionless, where $\langle S^z \rangle$ is the assembly statistical average of spin operator S^z. In calculation $J_1 = 1$ is fixed and J_2 varies.

We apply the double-time Green's-function method to deal with the Hamiltonian (2). The temperature-dependent retarded Green's function of operators A^+ and B^- is defined as [21]

$$G_{ij} = \ll A_i^+(t); e^{uB_j^z} B_j^- \gg = -i\theta(t)\langle [A_i^+(t); e^{uB_j^z} B_j^-] \rangle, \quad (3)$$

where $\theta(t)$ is the step function, and u is a parameter [21] (denoted by w in [22]). After the Fourier transformation, the Green's function observes the equation of motion:

$$\omega \ll A_i^+; e^{uB_j^z} B_j^- \gg = \langle [A_i^+; e^{uB_j^z} B_j^-] \rangle + \ll [A_i^+, H]; e^{uB_j^z} B_j^- \gg . \quad (4)$$

The high-order Green's function $\ll [A_i^+; H]; e^{uB_j^z} B_j^- \gg$ obeys an equation of motion that is similar to Eq. (4) with the higher-order Green's function appearing on the right-hand side. Thus a set of infinite coupled equations will be generated. To obtain tractable solutions, decoupling procedures have been invoked to terminate the hierarchy of the equations of motion. The RPA [21] is the decoupling usually taken. The Green's function can be Fourier transformed into k space:

$$G_{ij} = \frac{1}{N} \sum_k g(k,\omega) e^{ik\cdot(i-j)}, \quad (5)$$

where N is the number of lattice sites. The integral of the wave vector k extends over the first Brillouin zone. According to the standard spectral theorem, the correlation functions of the product of the spin operators can be calculated by the corresponding Green's function $g(k,\omega)$:

$$\langle e^{uB_j^z} B_j^- A_i^+ \rangle = \frac{i}{2\pi N} \sum_k e^{ik\cdot(i-j)} \times \int \frac{g(k,\omega + i0^+) - g(k,\omega - i0^+)}{e^{\beta\omega} - 1} d\omega. \quad (6)$$

Using the Callen method [21], we can obtain the average spin operator $m = \langle S^z \rangle$ and the ϕ_F function by means of the correlation function:

$$\phi_F = \langle e^{uB_j^z} B_j^- A_i^+ \rangle / \Theta(u), \quad F = \mathrm{AF1}, \mathrm{AF2}, \quad (7)$$

where $\Theta(u) = \langle [A_i^+; e^{uB_j^z} B_j^-] \rangle$ and $\Theta(u = 0) = 2m$. We skip the tedious derivation of magnetizations of AF1 and AF2 states. The self-consistent equation for computing magnetization can be expressed as [21]

$$m = \frac{(\phi_F + 1 + S)\phi_F^{2S+1} - (\phi_F - S)(\phi_F + 1)^{2S+1}}{(\phi_F + 1)^{2S+1} - \phi_F^{2S+1}}. \quad (8)$$

The expression of the ϕ_F function is

$$\phi_F = \frac{1}{N} \sum_k \frac{E_{1F}}{2\sqrt{E_{1F}^2 - E_{2F}^2}} \coth \frac{\beta\sqrt{E_{1F}^2 - E_{2F}^2}}{2} - \frac{1}{2}. \quad (9)$$

Here for the AF1 state

$$E_{1\mathrm{AF1}} = 4m[J_1 + J_2(\eta \cos k_x \cos k_y - 1)],$$
$$E_{2\mathrm{AF1}} = 2\eta m J_1(\cos k_x + \cos k_y), \quad (10)$$

and for the AF2 state

$$E_{1\mathrm{AF2}} = 2m[J_1 \eta \cos k_x + 2J_2],$$
$$E_{2\mathrm{AF2}} = 2\eta m(J_1 \cos k_y + J_2 \cos k_x \cos k_y). \quad (11)$$

III. RESULTS AND DISCUSSIONS

In this paper, we calculate the sublattice magnetizations at finite temperature. When we say zero temperature, we actually mean that temperature is very close to zero, which is denoted by $T = 0^+$. Figure 1 plots the magnetization dependent on temperature for different anisotropic parameters at $S = 1/2$. In Fig. 1(a), the magnetization decreases when J_2 approaches 1/2 from either side. This can be understood by the competition between J_1 and J_2. At $J_2 = \mathbf{0}$, it is an ordinary NN AF exchange system, i.e., AF1 state. As J_2 increases from zero, the frustration is induced. The competition between J_1 and J_2 emerges and becomes stronger with increasing the value of J_2. As a result, both T_N and m drop with increasing J_2 value. At $J_2 = 0.5$, the competition reaches the strongest. As J_2 increases further from 0.5, the effect of J_2 exchange becomes dominant, and the T_N and m increase with increasing J_2. In this case, the system is of AF2 configuration.

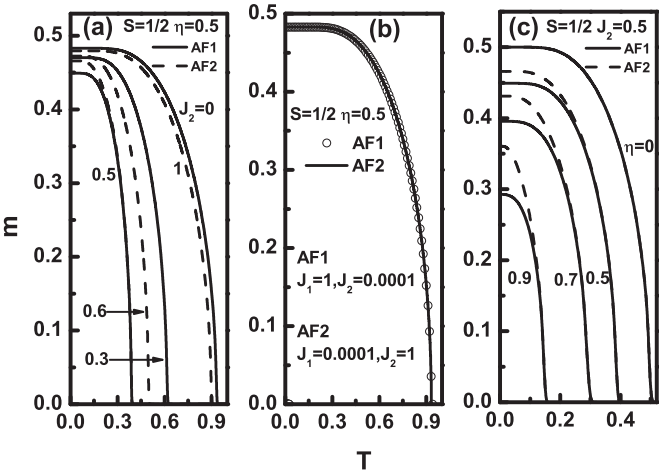

FIG. 1. The sublattice magnetization m as a function of temperature T at $S = 1/2$ under various parameters. (a) Anisotropy $\eta = 0.5$ and different J_2 values. (b) $\eta = 0.5$, $J_1 \gg J_2$, and $J_1 \ll J_2$. (c) $J_2 = 0.5$ and different η values. For $\eta = 0$, the two curves are identical.

Thus it is seen that the system is the AF1 state at $J_2 \leqslant 0.5$ and AF2 state at $J_2 \geqslant 0.5$, respectively. It indicates that the role of J_1 is the most important for $J_2 \ll 0.5$, while J_2 is predominant at $J_2 \gg 0.5$. In Fig. 1(b), we show the magnetization dependence on temperature for $J_1 \gg J_2$ or $J_1 \ll J_2$. It is seen that the curves of magnetization versus temperature are the same. This can be easily understood. In the former case, J_2 is very close to zero, and only the NN exchange J_1 plays a role. Hence the state is AF1 as has just been mentioned above. In the latter case, J_1 is close to zero. Imagine that if J_1=0 only the NNN exchange J_2 plays a role. In this case, the lattice can be partitioned into two independent sublattices, each being regarded as a square lattice with NN exchange J_2. Therefore, the two curves in Fig. 1(b) are identical. This conclusion stands for any anisotropy parameter $\eta < 1$.

It is noticed from Fig. 1(a) that at $J_2 = 0.5$ the two states have the same order-disorder transition point for anisotropic parameter $\eta = 0.5$. Let us see whether the conclusion is true for arbitrary anisotropy. Figure 1(c) plots the m-T curves for different anisotropic parameters at $J_2 = 0.5$. It is shown that the T_N for the AF1 and AF2 states are the same for any anisotropy $\eta < 1$. We have confirmed by our numerical evaluation that this conclusion is also valid for the spin quantum number $S > 1/2$. Hereafter, the magnetizations of AF1 and AF2 states at $T \to 0$ are denoted as $m_{\mathrm{AF1}}(0^+)$ and $m_{\mathrm{AF2}}(0^+)$, respectively. At each η value, the $m_{\mathrm{AF1}}(0^+)$ is lower than $m_{\mathrm{AF2}}(0^+)$. The reason is that in the AF1 configuration each spin is antiparallel to all of its four NN spins, while in the AF2 configuration each spin has two parallel and two antiparallel NN spins. Therefore, the AF1 state has stronger quantum fluctuation compared to the AF2 state. When $\eta = 0$, the magnetization curves of AF1 and AF2 are the same. This is because at $\eta = 0$ both AF1 and AF2 recover an ordinary two-dimensional Ising model. Therefore, as $T \to 0$, the sublattice magnetizations become fully saturated, $m(0^+) = S$, and there is no transversal quantum fluctuation. Figure 1(c) demonstrates two features as the η value decreases from one to zero. One is that both $m_{\mathrm{AF1}}(0^+)$ and $m_{\mathrm{AF2}}(0^+)$ increase until full saturation. The other is that the relative difference between $m_{\mathrm{AF1}}(0^+)$ and $m_{\mathrm{AF2}}(0^+)$ decreases. Both features are ascribed to the stronger transverse quantum fluctuation for smaller η value, or less anisotropy.

Figure 2 shows the order-disorder phase transition point T_N as a function of J_2 for $S = 1/2, 1, 3/2$ at several anisotropies η. These panels are also phase diagrams. Each solid line is the border line of paramagnetic and AF1 states, and each dashed line is the border line of paramagnetic and AF2 states, the paramagnetic phase being above the lines. It is seen that the critical temperature decreases with increasing η. It can be easily understood that the anisotropy suppresses the quantum fluctuation of the system, so that it leads to a large critical temperature. The three panels also exhibit that the solid and dashed lines with the same η value intersect at $J_2 = 0.5$, i.e., the AF1 and AF2 configurations with the same exchange anisotropy have the same critical temperatures as long as $J_2 = 0.5$. In the following, we study the cases where $J_2 = 0.5$. Since both states can exist under the conditions, one of them may be stabler.

To determine which state is stabler, evaluation of their thermodynamic functions is necessary. Under the same volume

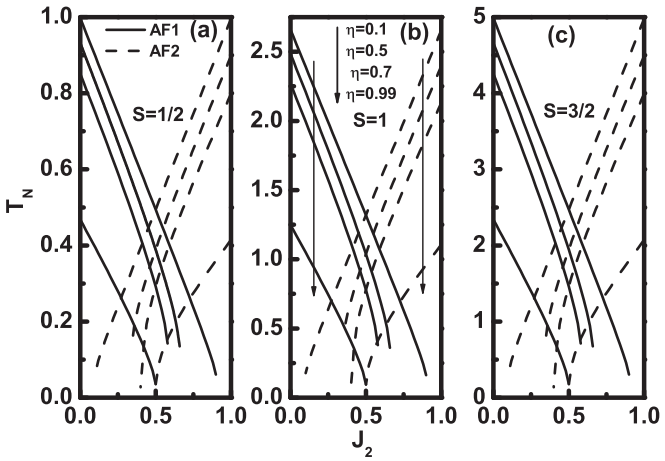

FIG. 2. The Néel temperature T_N as a function of J_2 at different S and η values. (a) $S = 1/2$. (b) $S = 1$. (c) $S = 3/2$.

and entropy, the state with lower internal energy is stabler. However, the entropies of the two states at a fixed temperature are different. Therefore, the internal energy is not a good judge function. Under the same volume and temperature, the state with lower free energy is stabler.

The free energy $F(T)$ can be evaluated numerically by means of the internal energy via $F(T) = E(0) - T\int_0^T \frac{E(T)-E(0)}{T^2} dT$, where the internal energy $E(T)$ is the thermostatistical average of the Hamiltonian, $E = \frac{<H>}{N}$ [21]. Therefore, before calculating the free energy, one has to compute the internal energy. Computing the internal energy involves the calculation of the transverse ($\sum_{i,j} < S_i^+ S_j^- >$) and longitudinal ($\sum_{i,j} < S_i^z S_j^z >$) correlation functions. The transverse correlation function can be directly calculated by use of the spectral theorem. For longitudinal correlation function, roughly, one may adopt the mean field approximation, i.e., $\sum_{i,j} < S_i^z S_j^z >= \sum_{i,j} < S_i^z >< S_j^z >$. A better expression for calculation of this term was given recently [23]. Here we follow the routine presented in [23] to calculate this part of energy.

Figure 3 plots the internal energies $E(T)$ and free energy $F(T)$ for different anisotropies at $S = 1/2$. The $E(T)$ increases with temperature as it should be. The free energy decreases monotonically with temperature. When $\eta = 0$, the $E(T)$ curves of the AF1 and AF2 are identical, and their $F(T)$ curves are as well [see Fig. 3(a)]. This is because the system with $\eta = 0$ is an Ising model, and there is no transverse quantum fluctuation, which has been mentioned in the interpretation of Fig. 1(c). In this case, the system has only a longitudinal correlation effect. As η increases from zero, the transverse correlation is induced.

To be explicit, at $T \to 0$ the internal energies of AF1 and AF2 states are denoted as $E_{\mathrm{AF1}}(0^+)$ and $E_{\mathrm{AF2}}(0^+)$, and their free energies are denoted as $F_{\mathrm{AF1}}(0^+)$ and $F_{\mathrm{AF2}}(0^+)$, respectively. When $\eta > 0$, the $m_{\mathrm{AF1}}(0^+)$ is different from $m_{\mathrm{AF2}}(0^+)$, as shown in Fig. 1(c). Correspondingly, their internal energies at $T \to 0$ are different from each other. However, when $\eta \leqslant 0.0637$, the difference is negligible, as shown by Fig. 3(b). We have evaluated that in this case $|(F_{\mathrm{AF2}} - F_{\mathrm{AF1}})/F_{\mathrm{AF2}}| < 0.0001$. It seems that the transverse

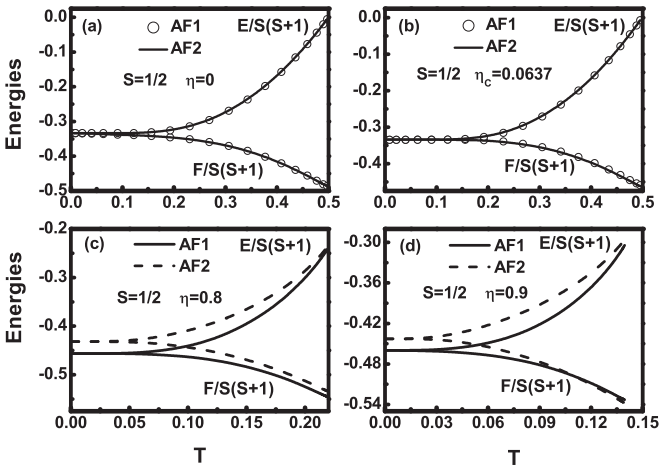

FIG. 3. The internal energies $E(T)$ (ascending curves) and free energies $F(T)$ (descending curves) as functions of the temperature T at $S = 1/2$ and different anisotropic parameters. (a) $\eta = 0$. (b) $\eta = 0.0637$. (c) $\eta = 0.8$. (d) $\eta = 0.9$.

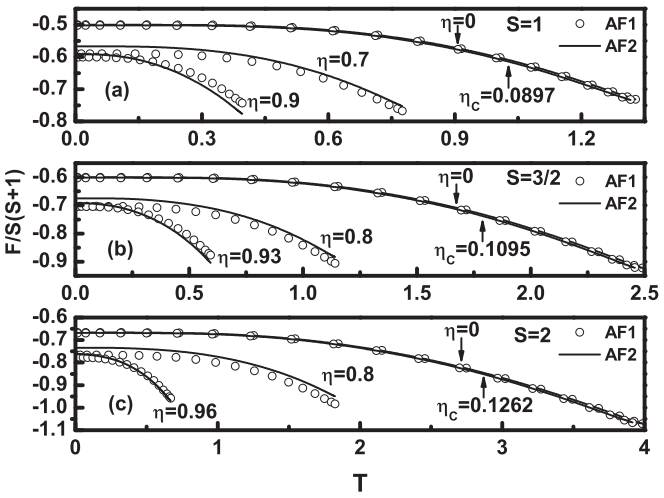

FIG. 4. The free energies $F(T)$ as a function of the temperature T at different S and η values. (a) $S = 1$. (b) $S = 3/2$. (c) $S = 2$.

correlation effect is so small that it is almost totally suppressed by the longitudinal correlation effect. The system can be either the AF1 or AF2 state, or coexistence of them.

When $\eta > 0.0637$, the transverse correlation effect becomes stronger, and the difference between the $E_{\mathrm{AF1}}(0^+)$ and $E_{\mathrm{AF2}}(0^+)$ becomes non-negligible. It is seen from Figs. 3(c) and 3(d) that $E_{\mathrm{AF1}}(0^+)$ is always lower than $E_{\mathrm{AF2}}(0^+)$, which coincides with the fact that $m_{\mathrm{AF1}}(0^+)$ is less than $m_{\mathrm{AF2}}(0^+)$. In Fig. 3, the free energies are plotted in the whole temperature range under T_N. In Figs. 3(c) and 3(d), the $F_{\mathrm{AF2}}(T)$ (descending dashed lines) decreases with temperature more rapidly than $F_{\mathrm{AF1}}(T)$ (descending solid lines). Figure 3(c) shows that $F_{\mathrm{AF1}}(T)$ is always lower than $F_{\mathrm{AF2}}(T)$ as $\eta = 0.8$. Hence, the AF1 state is stabler. As η further increases, the $F_{\mathrm{AF1}}(T)$ and $F_{\mathrm{AF2}}(T)$ curves can cross below the Néel point [see Fig. 3(d) as an example]. In this case, as temperature is close to zero, the system should be the AF1 state. As temperature rises, the $F_{\mathrm{AF1}}(T)$ and $F_{\mathrm{AF2}}(T)$ become closer, and at the cross point $F_{\mathrm{AF2}}(T)$ becomes lower than $F_{\mathrm{AF1}}(T)$. This means that the AF2 state becomes stabler. Therefore, there can occur an AF1-AF2 phase transition at the cross point. Above the transition point, the AF2 is stabler until the Néel point T_N.

Let us discuss the order of the transition. At the transition point, the free energies of the AF1 and AF2 states are the same, but their internal energies are different, as can be seen in Fig. 3(b). Subsequently, the specific heat at this point is discontinuous (not shown). Therefore, it is a first-order transition.

Figure 4 plots the free energy as a function of temperature for different anisotropy and S when J_2=0.5. For each spin quantum number, there is an η_C value. When $0 \leqslant \eta \leqslant \eta_C$, the difference between $F_{\mathrm{AF1}}(T)$ and $F_{\mathrm{AF2}}(T)$ is negligible. The η_C increases with increasing S. For $\eta > \eta_C$, $F_{\mathrm{AF1}}(0^+)$ is always lower than $F_{\mathrm{AF2}}(0^+)$. When η is up to 0.8 or so, $F_{\mathrm{AF1}}(T)$ is lower than $F_{\mathrm{AF2}}(T)$ within the whole temperature range below the Néel point, indicating that the AF1 state is stabler. When η rises further, say to about 0.9, the $F_{\mathrm{AF1}}(T)$ and $F_{\mathrm{AF2}}(T)$ have a cross, although the two curves are close to each other. In this case the system is the AF1 state in low temperature close to zero, and will transit to the AF2 state at some temperature below the Néel point. That is to say, a phase transition can occur and it is a first-order transition. This conclusion is valid for all calculated spin quantum numbers.

IV. CONCLUSIONS

We have investigated the J_1-J_2 Heisenberg model with exchange anisotropy on a square lattice, and focused on possible AF1-AF2 phase transition below the Néel point and its dependence on the exchange anisotropy. The exchange anisotropy is characterized by the parameter $0 \leqslant \eta \leqslant 1$, where $\eta = 0$ means an Ising model and $\eta \to 1$ tends to an isotropic Heisenberg model. When $J_2/J_1 = 0.5$, both AF1 and AF2 can exist, which raises a question of which one is stabler. This is judged by their free energies. For any spin quantum number S, there is an η_C value, below which the difference between the $F(T)$ of the two states is negligible. Therefore, either state can exist, and coexistence of them is possible. Above η_C, $F_{\mathrm{AF1}}(0^+)$ is always lower than $F_{\mathrm{AF2}}(0^+)$. In a wide range of η, $F_{\mathrm{AF1}}(T)$ is lower than $F_{\mathrm{AF2}}(T)$ in the whole temperature range below the Néel point. So, the state remains AF1 until the Néel point. As η is close to 1, there can occur a transition. As temperature is close to zero, the state is AF1, and near the Néel point the state is AF2, which is a first-order transition. This is ascribed to stronger transverse quantum fluctuation. The conclusion stands for any S value. The η_C value increases with spin quantum number S.

ACKNOWLEDGMENTS

This work was supported by the Natural Science Foundation of China (Grant No. 11404046), the Basic Research Foundation of Chongqing Education Committee of China (Grant No. KJ130615), and the Chongqing Science and Technology Committee of China (Grant No. cstc2014jcyjA50013).

[1] G. Misguich and C. Lhuillier, in *Frustrated Spin Systems*, edited by H. T. Diep (World Scientific, Singapore, 2004).
[2] A. S. T. Pires, Solid State Commun. **193**, 56 (2014).
[3] T. Roscilde, A. Feiguin, A. L. Chernyshev, S. Liu, and S. Haas, Phys. Rev. Lett. **93**, 017203 (2004).
[4] J. R. Viana and J. R. de Sousa, Phys. Rev. B **75**, 052403 (2007).
[5] H.-Y. Wang, Phys. Rev. B **86**, 144411 (2012).
[6] B. Abdelilah, B. Abdelrhani, and H. Ez-Zahraouy, Phys. Lett. A **238**, 398 (1998).
[7] R. F. Bishop, P. H. Y. Li, R. Darradi, J. Schulenburg, and J. Richter, Phys. Rev. B **78**, 054412 (2008).
[8] R. F. Bishop, P. H. Y. Li, D. J. J. Farnell, and C. E. Campbell, Phys. Rev. B **79**, 174405 (2009).
[9] R. F. Bishop, P. H. Y. Li, D. J. J. Farnell, and C. E. Campbell, Phys. Rev. B **82**, 024416 (2010).
[10] R. Darradi, J. Richter, J. Schulenburg, R. F. Bishop, and P. H. Y. Li, J. Phys.: Conf. Ser. **145**, 012049 (2009).
[11] R. Melzi, P. Carretta, A. Lascialfari, M. Mambrini, M. Troyer, P. Millet, and F. Mila, Phys. Rev. Lett. **85**, 1318 (2000).
[12] R. Darradi, O. Derzhko, R. Zinke, J. Schulenburg, S. E. Krüger, and J. Richter, Phys. Rev. B **78**, 214415 (2008).
[13] N. D. Mermin and H. Wagner, Phys. Rev. Lett. **17**, 1133 (1966).
[14] R. F. Bishop, D. J. J. Farnell, and J. B. Parkinson, Phys. Rev. B **58**, 6394 (1998).
[15] J. Richter and J. Schilenburg, Eur. Phys. J. B **73**, 117 (2010).
[16] J. Sirker, Z. Weihong, O. P. Sushkov, and J. Oitmaa, Phys. Rev. B **73**, 184420 (2006).
[17] T. Pardini and R. R. P. Singh, Phys. Rev. B **79**, 094413 (2009).
[18] T. Senthil, L. Balents, S. Sachdev, A. Vishwanath, and M. P. A. Fisher, Phys. Rev. B **70**, 144407 (2004).
[19] B. Schmidt, P. Thalmeier, and N. Shannon, Phys. Rev. B **76**, 125113 (2007).
[20] R. Nath, A. A. Tsirlin, H. Rosner, and C. Geibel, Phys. Rev. B **78**, 064422 (2008).
[21] P. Fröbrich and P. J. Kuntz, Phys. Rep. **432**, 223 (2006).
[22] Qing'an Li, Phys. Rev. B **70**, 014406 (2004).
[23] Huai-Yu Wang, Liang-Jun Zhai, and Meichun Qian, J. Magn. Magn. Mater. **354**, 309 (2014).